

Highlights from the observatories

Compiled by D. J. Saikia

Radio emission from pulsars

Radio emission from pulsars is believed to originate from ultrarelativistic particles streaming out along open field lines centred near the magnetic poles. Frequency dependence of pulsar emission could be valuable for constraining pulsar emission mechanisms and also probing the magnetosphere. Simon Johnston, Aris Karastergiou, Dipanjan Mitra and Yashwant Gupta have observed a total of 67 pulsars at five frequencies ranging from 243 to 3100 MHz using the GMRT at lower frequencies and the Parkes Telescope in Australia at higher frequencies. They suggest that the location of pulsar emission within the magnetosphere evolves with time as the pulsar spins down. In highly energetic pulsars, the emission comes from a confined range of high altitudes, in the middle range of spin down energies the emission occurs over a wide range of altitudes whereas in pulsars with low spin-down energies it is confined to low down in the magnetosphere (Johnston, Karastergiou, Mitra & Gupta 2008).

Nova RS Ophiuchi: first detection of emission at low radio frequencies

The binary system RS Ophiuchi consists of an M giant and a hot accreting white dwarf with an orbital period of 455.72 ± 0.83 days (Fekel et al. 2000 and references therein). The nova outbursts occur due to thermonuclear runaway on the surface of the white dwarf due to accretion of mass from the companion star (e.g. Kato 1990). Outbursts from this system have been recorded in 1898, 1933, 1958, 1967, and 1985 (cf. Rosino & Iijima 1987) and possibly in 1907 (Schaeffer 2004) and 1945 (Oppenheimer & Mattei 1993). Most recently, it was discovered to be in outburst on 2006 February 12.83 UT (Narumi et al. 2006), and it has been monitored extensively at a large number of wavelengths (O'Brien et al. 2006; Bode et al. 2006; Sokolowski et al. 2006; Das et al. 2006). Radio emission at high frequencies were detected 4.7 days after the outburst (Eyres et al. 2006), while high-resolution VLBI images at radio wavelengths showed the source to evolve from a ring to a complex multicomponent structure (O'Brien et al. 2006). Nimisha Kantharia,

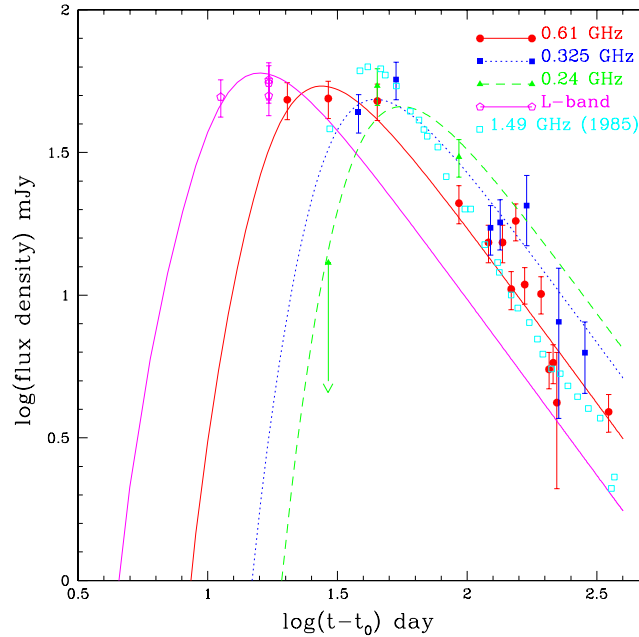


Figure 1. Observed light curves of RS Oph (points) at L-band, 0.61 GHz, 0.325 and 0.24 GHz observed in the 2006 outburst. Continuous lines represent the model light curves. Also plotted is the 1.49 GHz light curve from 1985 outburst.

G.C. Anupama and their collaborators have reported the first detection of this recurrent nova at frequencies less than 1400 MHz using the GMRT.

Radio emission was detected at 0.61 GHz on day 20 with a flux density of 48 mJy and at 0.325 GHz on day 38 with a flux density of 44 mJy. This is in contrast with the 1985 outburst, when it was not detected at 0.327 GHz even on day 66. The emission at low radio frequencies is nonthermal and is affected by foreground absorption due to the preexisting, ionized, warm, clumpy red giant wind. The absence of low-frequency radio emission in 1985 and the earlier turn-on of the radio flux in the current outburst are interpreted as being due to higher foreground absorption in 1985 compared to that in 2006 (Kantharia, Anupama, Prabhu, Ramya, Bode, Eyres & O'Brien 2007).

Supernovae studies with the HCT

SN 2005hk: The reasonable homogeneity in the light curves and peak luminosities of Type Ia supernovae (SNe Ia) make these good candidates for studying the extragalactic

distance scale. However, a number of these could also exhibit significant photometric and spectroscopic differences. The photometric and spectroscopic evolution of the type Ia supernova SN 2005hk was monitored during the pre-maximum to nebular phase using the 2m HCT. Observations in the nebular phase were also made using the 8m Subaru Telescope. The photometric and spectroscopic evolution indicate SN 2005hk to be peculiar, very different from normal type Ia SNe. SN 2005hk is found to be very similar to the peculiar Ia SN 2002cx. The bolometric light curve of SN 2005hk is characterized by its faintness at the maximum ($M_{bol} = -17.7$). This certainly indicates that only a small amount of ^{56}Ni is synthesized during the explosion. The slow decline rate of the light curve of SN 2005hk compared to normal SNe Ia indicates an explosion with lower kinetic energy. Also, the brightness at late phases indicates a more efficient trapping of the γ -rays from decaying ^{56}Co in SN 2005hk compared to normal SNe Ia such as SN 1992A. The pre-maximum spectra show a blue continuum, dominated by Fe III lines with weak Si II and Ca II H&K absorption, very similar to the over-luminous Ia SN 1991T. However, the photospheric velocities, measured based on the the absorption minimum corresponding to the Ca II H&K, Fe II, Fe III and Si II lines, indicate that SN 2005hk has much lower expansion velocities that decrease from $\sim 6900 \text{ km s}^{-1}$ on day -6 to $\sim 6200 \text{ km s}^{-1}$ on day -4 . This is consistent with the low kinetic energy estimates based on the light curve. The spectrum of SN 2005hk remained peculiar throughout. The nebular phase spectrum shows no signature of strong forbidden iron and cobalt lines that are seen in normal SNe Ia. On the contrary, SN 2005hk spectrum is dominated by Fe II lines and forbidden lines due to [Ca II] 7291, 7234 Å and lines due to [Fe II] at 7155 Å and 7453 Å. The presence of these lines is quite similar to what is observed in the late time spectra of SNe IIP (Sahu et al. 2008a).

SN 2007ru: The spectral evolution of the type Ic supernova SN 2007ru during the first 3 months show broad spectral features due to very high expansion velocity, normally seen in hypernovae. The photospheric velocity ~ 8 days after explosion is found to be lower than SN 1998bw, however, at later epochs it is comparable to that of SN 1998bw and higher than other type Ic supernovae. The light curve evolution of SN 2007ru indicates a fast rise time of 8 ± 3 days to B band maximum and post-maximum decline more rapid than other broad-line type Ic supernovae. With an absolute V magnitude of -19.10 , SN 2007ru is comparable in brightness with SN 1998bw and lies at the brighter end of the observed type Ic supernovae. The mass of ^{56}Ni is estimated to be $\sim 0.4 M_{\odot}$. The fast rise and decline of the light curve and the high expansion velocity suggest that SN 2007ru is an explosion with a high kinetic energy/ejecta mass ratio (E_K/M_{ej}). This adds to the diversity of type Ic supernovae. (Sahu, Tanaka, Anupama, Gurugubelli & Nomoto 2008b).

FIGGS: Faint Irregular Galaxies GMRT Survey

The Faint Irregular Galaxies GMRT Survey (FIGGS) is a GMRT based HI imaging survey of a systematically selected sample of extremely faint nearby dwarf irregular galaxies.

The primary goal of FIGGS is to provide a comprehensive and statistically robust characterization of the neutral interstellar medium properties of faint, gas-rich dwarf galaxies. The FIGGS galaxies represent the extremely low mass end of the dwarf irregular galaxies population, with a median $M_B \sim -13.0$ and median HI mass of $\sim 3 \times 10^7 M_\odot$, extending the baseline in mass and luminosity space for a comparative study of galaxy properties. From the FIGGS data, Ayesha Begum and her collaborators find that to a good approximation, the discs of gas-rich galaxies, ranging over three orders of magnitude in HI mass, can be described as being drawn from a family with fixed HI average surface density (Begum, Chengalur, Karachentsev, Sharina & Kaisin 2008).

Ayesha Begum and her collaborators also study Tully-Fisher (TF) relations for a sample that combines extremely faint galaxies drawn from FIGGS along with bright galaxies. For the faint galaxies, they find that the HI mass correlates significantly better with the circular velocity indicators than the stellar mass. The faint galaxies lie systematically below the I-band TF relation defined by bright galaxies, and also show significantly more intrinsic scatter. This implies that the integrated star formation in these galaxies has been both less efficient and also less regulated than in large galaxies (Begum, Chengalur, Karachentsev & Sharina 2008).

The Local Group dwarf Leo T: HI on the brink of star formation

Leo T, a member of the Local Group, is amongst the lowest luminosity galaxies with on-going star formation (Irwin et al. 2007). It is a complex dwarf galaxy whose colour-magnitude diagram reveals both a red giant branch and young blue stars with ages of ~ 68 Gyr and 200 Myr respectively. Located about 420 kpc from the Milky Way, Leo T appears to have associated HI gas in the Northern HI Parkes All-Sky Survey (HIPASS, Wong et al. 2006). Studies of such small dwarf galaxies could provide valuable insights into how the least massive dark matter halos retain gas and form stars. Emma Ryan-Weber and her collaborators present GMRT and WSRT observations of Leo T. The peak HI column density is measured to be $7 \times 10^{20} \text{ cm}^{-2}$, and the total HI mass is $2.8 \times 10^5 M_\odot$. Leo T has both cold (~ 500 K) and warm (~ 6000 K) HI at its core, with a global velocity dispersion of 6.9 km s^{-1} , from which they derive a dynamical mass within the HI radius of $3.3 \times 10^6 M_\odot$, and a mass-to-light ratio of >50 . They find that the gas should be globally stable against star formation. Leo T appears to be the most dark matter-dominated, gas-rich dwarf in the Local Group (Ryan-Weber, Begum, Oosterloo, Pal, Irwin, Belokurov, Evans & Zucker 2008).

HI gas at moderate redshifts

The cosmic density of neutral gas is not well constrained between the present time and redshifts of ~ 1 , although the cosmic star formation rate is known to increase by about an order of magnitude over this redshift range (Lilly et al. 1996; Madau et al. 1996; Hopkins

2004). Constraining the evolution of neutral gas would be an important input towards our understanding of star formation and galaxy evolution. However, this is usually difficult from HI 21-cm emission observations because the flux density of individual galaxies is usually below the detection limits of present telescopes for reasonable observing times. Philip Lah and his collaborators have used the GMRT to measure the HI gas content of star-forming galaxies at $z = 0.24$ (i.e. a look-back time of ~ 3 Gyr). The sample of galaxies studied was selected from H α -emitting field galaxies detected in a narrow-band imaging survey with the Subaru Telescope. The Anglo-Australian Telescope was used to obtain precise optical redshifts for these galaxies. They then co-added the HI 21-cm emission signal for all the galaxies within the GMRT spectral line data cube. From the co-added signal of 121 galaxies, they measure an average atomic hydrogen gas mass of $2.26 \pm 0.90 \times 10^9 M_{\odot}$. They translate this HI signal into a cosmic density of neutral gas at $z = 0.24$ of $\Omega_{\text{gas}} = (0.91 \pm 0.42) \times 10^{-3}$. This value is consistent with that estimated from damped Ly α systems around this redshift. They also find that the correlations between the H α luminosity and the radio continuum luminosity and between the star formation rate (SFR) and the HI gas content in star-forming galaxies at $z = 0.24$ are consistent with the correlations found at $z = 0$. These two results suggest that the star formation mechanisms in field galaxies ~ 3 Gyr ago were not substantially different from the present, even though the SFR is three times higher (Lah et al. 2007). It is relevant to note that from deep integrations with the Westerbork Synthesis Radio Telescope of two galaxy clusters at redshifts of about 0.2, Verheijen et al. (2007) reported HI detections from 42 galaxies, with HI masses in the range of 5×10^9 to $4 \times 10^{10} M_{\odot}$.

Outflowing atomic and molecular gas at $z \sim 0.67$ towards 1504 + 377

This is an interesting and rare example of a radio-loud AGN being hosted by a disk galaxy (e.g. Perlman et al. 1996; Carilli et al. 1997). The quasar has a compact flat-spectrum core and a one-sided jet to the south-west (Polatidis et al. 1995; Fomalont et al. 2000). The AGN appears heavily reddened ($r-K=5.1$). Nissim Kanekar and Jayaram Chengalur report the detection of OH 1667-MHz and wide HI 21-cm absorption at $z \sim 0.67$ towards 1504+377, with the GBT and the GMRT. The HI 21-cm absorption extends over a velocity range of $\sim 600 \text{ km s}^{-1}$ blueward of the quasar redshift ($z = 0.674$), with the new OH 1667-MHz absorption component at $\sim 430 \text{ km s}^{-1}$, nearly coincident with earlier detections of millimetre-wave absorption at $z \sim 0.6715$. The atomic and molecular absorption appear to arise from a fast gas outflow from the quasar. The radio structure is consistent with the outflow arising as a result of a jet-cloud interaction, followed by rapid cooling of the cloud material. The observed ratio of HCO+ and OH column densities is ~ 20 times higher than typical values in Galactic and high- z absorbers. This could arise because of small-scale structure in the outflowing gas on sub-parsec scales, which would also explain the observed variability in the HI 21-cm line (Kanekar & Chengalur 2008).

Dusty 21-cm absorbers at $z \sim 1.3$

Studying the physical conditions in the interstellar medium (ISM) at high redshift and the processes that maintain these conditions is important for our understanding of how galaxies form and evolve. Raghunathan Srianand and his collaborators have discovered two dusty intervening Mg II absorption systems at $z \sim 1.3$ in the Sloan Digital Sky Survey (SDSS) database. The overall spectra of both QSOs are red ($u-K > 4.5$ mag) and are well modelled by the composite QSO spectrum reddened by the extinction curve from the Large Magellanic Cloud (LMC2) Supershell redshifted to the rest-frame of the Mg II systems. In particular, they detect clearly the presence of the UV extinction bump at $\lambda_{\text{rest}} \sim 2175$ Å. Absorption lines of weak transitions like Si II $\lambda 1808$, Cr II $\lambda 2056$, Cr II + Zn II $\lambda 2062$, Mn II $\lambda 2594$, Ca II $\lambda 3934$ and Ti II $\lambda 1910$ from these systems are detected even in the low signal-to-noise ratio and low resolution SDSS spectra, suggesting high column densities of these species. The depletion pattern inferred from these absorption lines is consistent with that seen in the cold neutral medium of the LMC. Using the LMC A_V vs. $N(\text{H I})$ relationship we derive $N(\text{H I}) \sim 6 \times 10^{21} \text{ cm}^{-2}$ in both systems. Metallicities are close to solar. GMRT observations of these two relatively weak radio loud QSOs ($f_\nu \sim 50$ mJy) resulted in the detection of 21-cm absorption in both cases. We show that the spin temperature of the gas is of the order of or smaller than 500 K (Srianand, Gupta, Petitjean, Noterdaeme & Saikia 2008).

HI 21-cm absorption at $z \sim 3.39$

High-redshift damped Ly α absorbers (DLAs), are possibly the precursors of today's galaxies (e.g. Wolfe, Gawiser & Prochaska 2005), and understanding their evolution could provide valuable insights towards understanding galaxy evolution. Nissim Kanekar, Jayaram Chengalur and Wendy Lane report the GMRT detection of HI 21-cm absorption from the $z \sim 3.39$ DLA towards PKS 0201+113, the highest redshift at which 21-cm absorption has been detected in a DLA. The absorption is spread over $\sim 115 \text{ km s}^{-1}$ and has two components, at $z = 3.387144(17)$ and $z = 3.386141(45)$.

They model the 21-cm absorbing gas as having a two-phase structure with cold dense gas randomly distributed within a diffuse envelope of warm gas. For such a model, their radio data indicate that, even if the optical QSO lies along a line of sight with a fortuitously high (50 per cent) cold gas fraction, the average cold gas fraction is low, < 17 per cent, when averaged over the spatial extent of the radio core (Kanekar, Chengalur & Lane 2007).

The largest giant radio galaxy and an unusual large radio jet

Jerzy Machalski and his collaborators have reported the discovery of the largest giant radio galaxy known, J1420–0545: an FR type II radio source with an angular size of 17.4

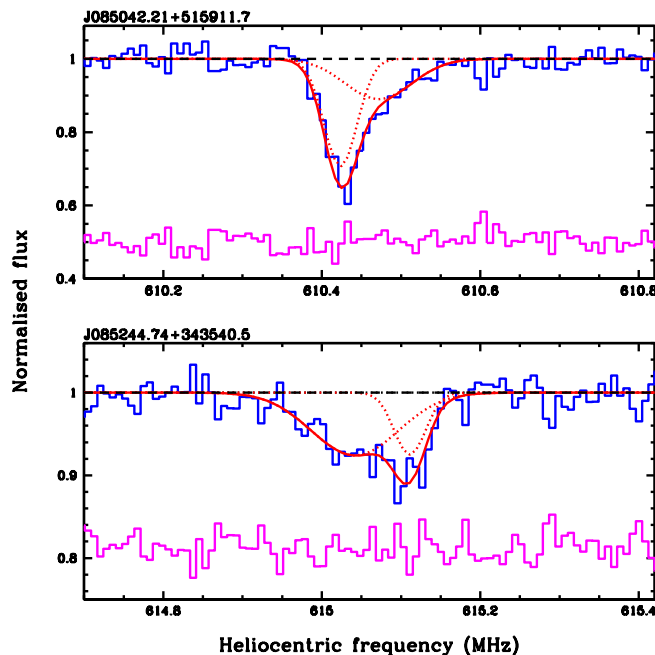


Figure 2. GMRT spectra of J085042.21+515911.7 (top panel) and J085244.74+343540.5 (bottom panel). H I 21-cm absorption is detected at $z_{\text{abs}} \approx 1.3265$ and 1.3095 respectively. The solid lines represent the fits to the overall profiles. Individual Gaussian components are shown with dotted lines. Residuals, on a scale arbitrarily shifted for clarity, are also plotted.

arcmin, identified with an optical galaxy at $z=0.3067$. Thus, the projected linear size of the radio structure is 4.69 Mpc ($H_0=71 \text{ km s}^{-1} \text{ Mpc}^{-1}$, $\Omega_m=0.27$, $\Omega_{vac}=0.73$). This makes it larger than 3C 236, which is the largest double radio source known to date. New radio observations with the 100 m Effelsberg telescope and the GMRT, as well as optical identification with a host galaxy and its optical spectroscopy with the William Herschel Telescope, have been reported. The spectrum of J1420-0545 is typical of elliptical galaxies in which continuum emission with the characteristic 4000 Å discontinuity and the H and K absorption lines are dominated by evolved stars. The dynamical age of the source, its jets' power, the energy density, and the equipartition magnetic field are calculated and compared with the corresponding parameters of other giant and normal-sized radio galaxies from a comparison sample. The source is characterized by the exceptionally low density of the surrounding IGM and an unexpectedly high expansion speed of the source along the jet axis. All of these may suggest a large inhomogeneity of the IGM (Machalski, Kozieł-Wierzbowska, Jamroz & Saikia 2008).

Joydeep Bagchi and his collaborators have reported the discovery of a very unusual,

highly asymmetric radio galaxy whose radio jet is the largest. The radio galaxy emits strongly polarized synchrotron radiation and can be traced all the way from the galactic nucleus to the hot spot located ~ 440 kpc away. This jet emanates from an extremely massive black hole ($>10^9 M_{\odot}$) and forms a strikingly compact radio lobe. No radio lobe is detected on the side of the counterjet, even though it is similar to the main jet in brightness up to a scale of tens of kiloparsecs. Thus, contrary to the nearly universal trend, the brightness asymmetry in this radio galaxy increases with distance from the nucleus. With several unusual properties, including a predominantly toroidal magnetic field, this Fanaroff- Riley type II megajet is an exceptionally useful laboratory for testing the role of magnetic field in jet stabilization and radio lobe formation (Bagchi, Gopal-Krishna, Krause & Joshi 2007).

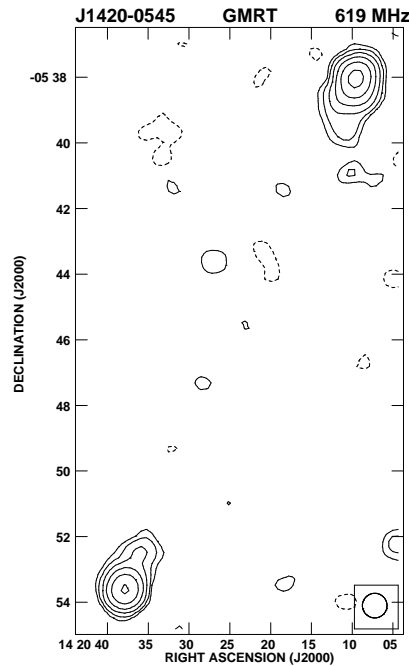


Figure 3. GMRT image of the largest giant radio galaxy at 619 MHz.

Optical afterglow of GRB 050319: The wind-to-ISM transition in view

The collapse of a massive star is believed to be the most probable progenitor of a long gamma-ray burst (GRB). Such a star is expected to have its environment modified by

the stellar wind. The effect of such a circumstellar wind medium is expected to be seen in the evolution of a GRB afterglow, but so far this has not been conclusively found. Atish Kamble, L.Resmi and Kuntal Misra claim that a signature of the transition from wind to constant density medium of the circumburst medium is visible in the afterglow of GRB 050319. Optical CCD observations of the afterglow of GRB 050319 were carried out in Johnson BV and Cousins RI filters using the 104 cm Sampurnanand Telescope of ARIES. Along with the optical observations of the afterglow of GRB 050319, they present a model for the multiband afterglow of GRB 050319. They show that the break seen in the optical light curve at ~ 0.02 days could be explained as being due to the transition from wind to constant density medium of the circumburst medium, in which case, this appears to be the first ever detection of such a transition at any given frequency band. Detection of such a transition could also serve as confirmation of the massive star collapse scenario for GRB progenitors, independent of supernova signatures (Kamble, Resmi & Misra 2007).

References

- Bagchi, J., Gopal-Krishna, Krause, M., & Joshi, S., 2007, *ApJ*, 670, 85L
 Begum, A., Chengalur, J.N., Karachentsev, I.D., & Sharina, M.E., 2008, *MNRAS*, 386, 138
 Begum, A., Chengalur, J.N., Karachentsev, I.D., Sharina, M.E., & Kaisin, S.S., 2008, *MNRAS*, 386, 1667
 Bode, M.F., et al., 2006, *ApJ*, 652, 629
 Carilli, C.L., Menten, K.M., Reid, M.J., & Rupen, M.P., 1997, *ApJ*, 474, 89L
 Das, R., Banerjee, D.P.K., & Ashok Nagarhalli, M., 2006, *ApJ*, 653, 141L
 Eyres, S.P.S., O'Brien, T.J., Muxlow, T.W.B., Bode, M.F., & Evans, A., 2006, *IAUC*, 8678, 2
 Fekel, F.C., Joyce, R.R., Hinkle, K.H., & Skrutskie, M.F., 2000, *AJ*, 119, 1375
 Fomalont, E.B., Frey, S., Paragi, Z., Gurvits, L.I., Scott, W.K., Taylor, A.R., Edwards, P.G., & Hirabayashi, H., 2000, *ApJS*, 131, 95
 Hopkins, A.M., 2004, *ApJ*, 615, 209
 Irwin, M.J., et al., 2007, *ApJL*, 656, 13L
 Johnston, S., Karastergiou, A., Mitra, D., & Gupta, Y., 2008, *MNRAS*, 388, 261
 Kamble, A., Resmi, L., & Misra, K., 2007, *ApJ*, 664, L5
 Kanekar, N., & Chengalur, J.N., 2008, *MNRAS*, 384, 6L
 Kanekar, N., Chengalur, J.N., & Lane, W.M., 2007, *MNRAS*, 375, 1528
 Kantharia, N.G., Anupama, G.C., Prabhu, T.P., Ramya, S., Bode, M.F., Eyres, S.P.S., & O'Brien, T.J., 2007, *ApJL*, 667, 171
 Kato, M., 1990, *ApJ*, 355, 277
 Lah, P., et al., 2007, *MNRAS*, 376, 1357
 Lilly, S.J., Le Fevre, O., Hammer, F., & Crampton, D., 1996, *ApJ*, 460, 1L
 Machalski, J.; Koziel-Wierzbowska, D., Jamrozy, M., & Saikia, D.J., 2008, *ApJ*, 679, 149
 Madau, P., Ferguson, H.C., Dickinson, M.E., Giavalisco, M., Steidel, C.C., & Fruchter, A., 1996, *MNRAS*, 283, 1388
 Narumi, H., Hirose, K., Kanai, K., Renz, W., Pereira, A., Nakano, S., Nakamura, Y., & Pojmanski, G., 2006, *IAUC*, 8671, 2
 O'Brien, T.J., Bode, M. F., Porcas, R.W., Muxlow, T.W.B., Eyres, S.P.S., Beswick, R.J., Garington, S.T., Davis, R.J., & Evans, A., 2006, *Nature*, 442, 279

- Oppenheimer, B.D., & Mattei, J.A., 1993, JAVSO, 22, 105
- Perlman, E.S., Carilli, C.L., Stocke, J.T., & Conway, J., 1996, AJ, 111, 1839
- Polatidis, A.G., Wilkinson, P.N., Xu, W., Readhead, A.C.S., Pearson, T.J., Taylor, G.B., & Vermeulen, R.C., 1995, ApJS, 98, 1
- Rosino, L., & Iijima, T., 1987, in RS Ophiuchi (1985) and the Recurrent Nova Phenomenon, Proceedings of the Manchester Conference, edited M.F. Bode, Utrecht: VNU Science Press, p.27
- Ryan-Weber, E.V., Begum, A., Oosterloo, T., Pal, S., Irwin, M.J., Belokurov, V., Evans, N.W., & Zucker, D.B., 2008, MNRAS, 384, 535
- Sahu, D.K., et al., 2008a, ApJ, 680, 580
- Sahu, D.K., Tanaka, M., Anupama, G.C., Gurugubelli, U.K., & Nomoto, K., 2008b, ApJL, submitted (arXiv:0805.3201)
- Schaefer, B.E., 2004, IAUC, 8396, 2
- Sokoloski, J.L., Luna, G.J.M., Mukai, K., & Kenyon, S.J., 2006, Nature, 442, 276
- Srianand, R., Gupta, N., Petitjean, P., Noterdaeme, P., & Saikia, D.J., 2008, MNRAS Letters, in press, (arXiv:0809.0919)
- Verheijen, M., van Gorkom, J.H., Szomoru, A., Dwarakanath, K.S., Poggianti, B.M., & Schiminovich, D., 2007, ApJ, 668, 9L
- Wolfe, A.M., Gawiser, E., & Prochaska, J.X., 2005, ARA&A, 43, 861
- Wong, O.I., et al., 2006, MNRAS, 371, 1855